

Texture analysis as a marker for identifying joint changes in temporomandibular disorders on magnetic resonance imaging

Análise de textura como marcador para identificação de alterações das articulares por disfunções temporomandibulares em imagens por ressonância magnética

Victoria Geisa Brito de OLIVEIRA¹ , Elaine Cristina de Carvalho Beda Correa de ARAUJO¹ , André Luiz Ferreira COSTA² , Michelle Bianchi de MORAES¹ , Sérgio Lucio Pereira de Castro LOPES¹ 

1 - Universidade Estadual Paulista “Júlio de Mesquita Filho”, Instituto de Ciência e Tecnologia, Departamento de Diagnóstico e Cirurgia. São José dos Campos, SP, Brazil.

2 - Universidade Cruzeiro do Sul, Programa de Pós-graduação em Odontologia. São Paulo, SP, Brazil.

How to cite: Oliveira VGB, Araujo ECCBC, Costa ALF, Moraes MB, Lopes SLP. Texture analysis as a marker for identifying joint changes in temporomandibular disorders on magnetic resonance imaging. *Braz Dent Sci*. 2024;27(3):e4312. <https://doi.org/10.4322/bds.2024.e4312>

ABSTRACT

Objective: The present investigation aimed to characterize Texture Analysis (TA) parameters of the condylar medullary bone and the superior aspect of the lateral pterygoid muscle (LPM) on Magnetic Resonance Imaging (MRI) for the identification of potential changes in individuals with temporomandibular disorder (TMD).

Material and Methods: A total of 40 MRI scans was retrospectively selected, consisting of 20 from patients without temporomandibular joint (TMJ) changes (control group) and 20 from patients diagnosed with TMD (TMD group). All MRI scans adhered to a consistent protocol, utilizing an 8.0 cm diameter bilateral surface coil to capture latero-medial parasagittal images with T2-weighted and Proton Density-weighted (PD), both with the mouth closed and at maximum mouth opening. TA was performed using the MaZda 4.20 software (Institute of Electronics, Technical University of Lodz, Poland). The regions of interest (ROI) were standardized for all evaluated images, and texture parameters were calculated through the gray-level co-occurrence matrix method. TA results underwent comparison using the Mann-Whitney test. **Results:** There was a statistically significant difference in the Correlation and Moment of Inverse Difference parameters between control and TMD groups, notably evident in PD-weighted images for the region of the condylar medullary bone and the LPM, respectively ($p<0.05$). **Conclusion:** Thus, the TA method exhibits promising potential to provide valuable information, enhancing the accuracy of TMD diagnosis and classification.

KEYWORDS

Dentistry; Diagnostic imaging; Magnetic resonance imaging; Radiomics; Temporomandibular joint dysfunction syndrome

RESUMO

Objetivo: Objetivou-se caracterizar os parâmetros de AT da medular do côndilo e do ventre superior do músculo pterigóideo lateral (MPL) em imagens de Ressonância Magnética (RM), com o intuito de identificar possíveis alterações de indivíduos com disfunção temporomandibular (DTM). **Material e Métodos:** Foram selecionados 40 exames de RM das articulações temporomandibulares de arquivo, sendo 20 exames de pacientes sem alteração na articulação temporomandibular (ATM) (grupo C) e 20 exames de indivíduos diagnosticados com disfunção temporomandibular (grupo DTM). Todos os exames de RM foram adquiridos com o mesmo protocolo, utilizando uma bobina de superfícies bilaterais de 8,0 cm de diâmetro, com imagens parassagitais látero-mediais, ponderadas em T2 e Densidade Protônica (DP), em boca fechada e máxima abertura bucal. Para a AT utilizou-se o software MaZda 4.20 (Institute of Electronics, Technical Universityof Lodz, Polônia), foram determinadas as regiões de interesse (ROIs), sendo a mesma para todas as imagens e, então, foram calculados os parâmetros de textura,

por meio do método de matriz de co-ocorrência de níveis de cinza. Os resultados foram submetidos ao teste de Mann-Whitney. **Resultados:** Pôde-se verificar que os parâmetros de Correlação e de Momento da Diferença Inversa apresentaram diferença estatisticamente significante, entre os grupos analisados C x DTM verificados nas imagens ponderadas em DP, para a região da medular condilar e do MPL, respectivamente ($p<0.05$). **Conclusão:** A AT é um método que tem potencial para fornecer informações com a finalidade de melhorar a precisão do diagnóstico e da classificação das DTM.

PALAVRAS-CHAVE

Odontologia; Diagnóstico por imagem; Ressonância magnética; Radiômica; Síndrome da disfunção temporomandibular

INTRODUCTION

The temporomandibular joints (TMJs) are diarthrodial synovial joints that interface with the temporal bone, a constituent of the fixed skull, and the mandible [1]. The complex dynamics of TMJs, coupled with their interaction with the stomatognathic system, render them susceptible to pathological changes. Temporomandibular disorders (TMD) represent a term employed to describe clinical alterations encompassing the TMJs, masticatory muscles, and other structures linked to the TMJs [2].

TMD stand out as the most common instances of non-dental chronic orofacial pain encountered by dentists and other healthcare professionals [3]. The etiology of TMD is multifactorial, encompassing a range of biological, environmental, and biopsychosocial factors [4,5]. Consequently, the diagnosis of these disorders plays a crucial role in dental practice, given their significant impact on the quality of life for patients experiencing TMD-related disturbances.

In this context, magnetic resonance imaging (MRI) is recognized as the gold standard for visualizing anatomical structures of the TMJ [6,7]. When assessing the TMJ, MRI not only proves to be a non-invasive examination, owing to the absence of ionizing radiation, but it is also the exclusive imaging modality that allows visualization of the fibrocartilaginous articular disc. This capability facilitates the examination of its position, shape, potential signal alterations, and function, while delivering high-resolution images for muscular tissues [8,9]. Moreover, the weighting of images during acquisition, whether in T1, T2, or proton density (PD), enables comparative studies of tissue behavior, thereby aiding in the identification of changes such as avascular necrosis and medullary

edema, which are characteristics inherently revealed by MRI [10].

Texture analysis (TA) is an advanced image processing technique that extracts pertinent features by delving into the intricacies of existing texture patterns [11,12]. Texture can be understood as intrinsic characteristics of the image (e.g. brightness, color, and shape distribution) that convey the idea of regularity, roughness, smoothness, among others, hence the name texture. This technique can be applied for efficient image classification, relying on parameters, or in discerning subtle variations within its gray values distribution [13]. Various approaches exist for extracting texture parameters from an image, and in the field of medical images, the statistical approach, including the Gray-Level Co-occurrence Matrix (GLCM), stands out as one of the most commonly employed methods [11,13-15].

TA emerges as a promising method for scrutinizing image data, with the potential to significantly improve diagnostic capabilities. This methodology entails the automated measurement of pixel intensity variation, thereby offering deeper insights into disease progression [16,17]. Within this framework, TA has garnered increasing attention in prior investigations, exemplified by its application in the identification and diagnosis of conditions such as breast tumors, brain tumors, muscular dystrophies, epilepsy, mild cognitive impairment, attention deficit, and the analysis of altered function in the lateral pterygoid muscle (LPM) in TMD [18-23].

Hence, the aim of this study was to apply the TA technique to analyze potential alterations in the condylar medullary bone and LPM in patients with TMD using MRI scans. The null hypothesis of this study is that the TA technique isn't effective in

analyzing possible changes in the aforementioned structures through MRI in patients with TMD.

MATERIAL AND METHODS

Ethical aspects

This study, characterized as observational, retrospective, and cross-sectional, was conducted at the Dentomaxillofacial Radiology and Imaging Clinic (Department of Diagnosis and Surgery) at the School of Dentistry of the Institute of Science and Technology of São Paulo State University (ICT UNESP) in São José dos Campos, São Paulo, Brazil.

Approval for the study was obtained from the Ethics Committee on Human Research of the aforementioned institution, adhering to the guidelines outlined in Resolution number 196/96, with protocol number CAAE: 32339720.8.0000.0077.

Characterization and sample selection

The non-probabilistic sample was obtained through convenience sampling and based on the study by Fardim et al. [24]. Clinical data and TMJ MRI scans, previously obtained and stored in the database of the Radiology Clinic OF the Department of Diagnosis and Surgery at the School of Dentistry in São José dos Campos (ICT UNESP), were recruited. A sample of 40 patients was considered, categorized into groups based on individuals' alterations represented by TMJ MRI scans. Twenty MRI scans were selected from individuals without TMD or any other alterations in the TMJ (Control Group), and another 20 MRI scans were chosen from individuals diagnosed with TMD (TMD Group). These patients were within the age range of 16 to 71 years, with a mean age of 38.91 ± 17.02 years.

The diagnosis of TMD was determined immediately before the time of MRI acquisition, with both groups undergoing a clinical examination of the TMJ conducted by an experienced specialist in orofacial pain. The examination adhered to the Research Diagnostic Criteria for Temporomandibular Disorders (RDC/TMD) as outlined by Dworkin et al. [25].

Sample categorization

The sample comprised 40 patients, divided into two groups (Control and TMD Groups). MRI images for analysis were acquired with T2 and PD

weighting, aligning with the predefined groups for the study, resulting in a total of 80 TMJs.

Inclusion criteria for sample selection involved scans meeting basic requirements and providing clear visualization of the condylar structures and LPM. Exclusion criteria encompassed scans with artifacts hindering the determination of TMJ anatomical structures and those displaying degenerative condylar changes such as erosion, flattening, and osteophytes.

All analyses were performed by an oral radiologist with over 5 years of experience in TMJ MRI image evaluation. To ensure calibration, TA was conducted on 10% of the sample. Subsequently, the analysis was repeated after 15 days, and the Intraclass Correlation Coefficient (ICC) was applied until achieving excellent agreement.

For each image, two Regions of Interest (ROIs) were established, one in the condylar medullary bone and another in the LPM (Figures 1 and 2). The distribution of groups is presented in Tables I and II based on the weighting of each image and the location of ROIs.

The parasagittal (i.e. oblique sagittal) reconstructions perpendicular to the long axes of the mandibular condyles were analyzed, as seen in Figure 1 and 2.

Texture analysis

After obtaining and processing the MRI scans, they were exported in DICOM (Digital Imaging and Communications in Medicine) format using OnDemand3D software (Cybermed Inc., Tustin, CA, USA), and subsequently converted to bitmap (BMP) format. All BMP images were then imported into MaZda 4.20 software (Institute of Electronics, Technical University of Lodz, Poland), a specialized and freely available package designed for TA purpose [26-28]. Introduced in 1998, this software was initially developed for TA in MRI but has versatility across various image modalities, including intraoral radiographs [29] and Cone beam Computed Tomography (CBCT) [30,31].

The TA process involves manually delineating ROIs using the available delineation tools in the software. The software automatically performed mathematical calculations and generated recorded features of these regions based on the tissues within the ROIs. This process utilizes a single slice for each ROI, as illustrated in Figures 1 and 2.

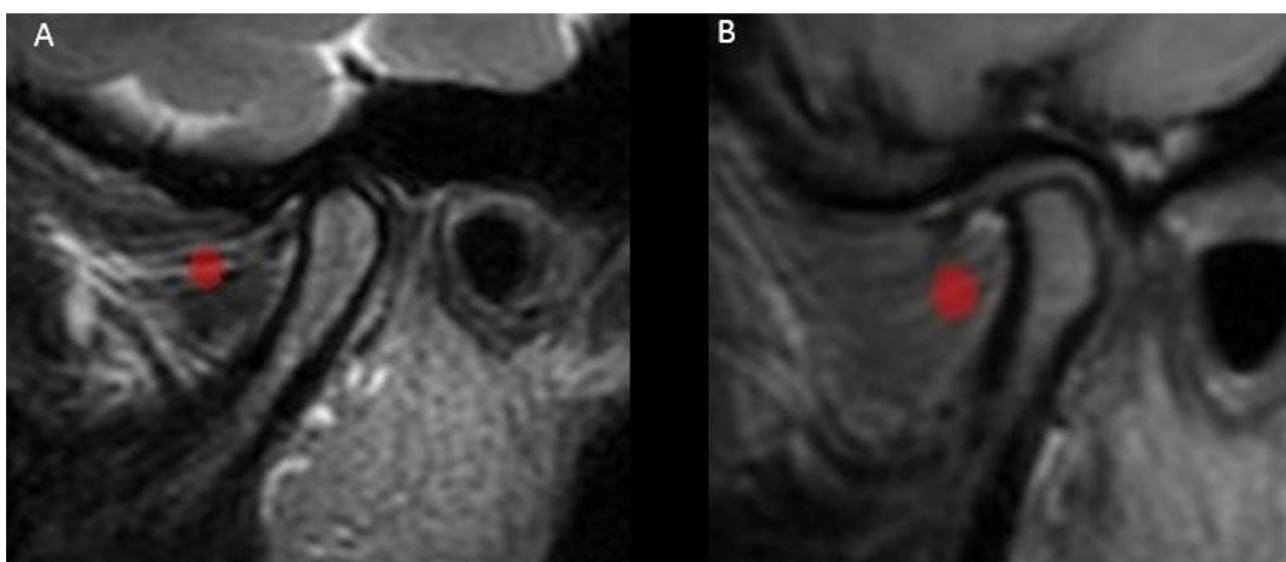


Figure 1 - Regions of Interest (ROIs) established in the condylar medullary bone in T2-weighted (A) and PD-weighted (B) magnetic resonance imaging reconstructions. Source: Prepared by the authors.

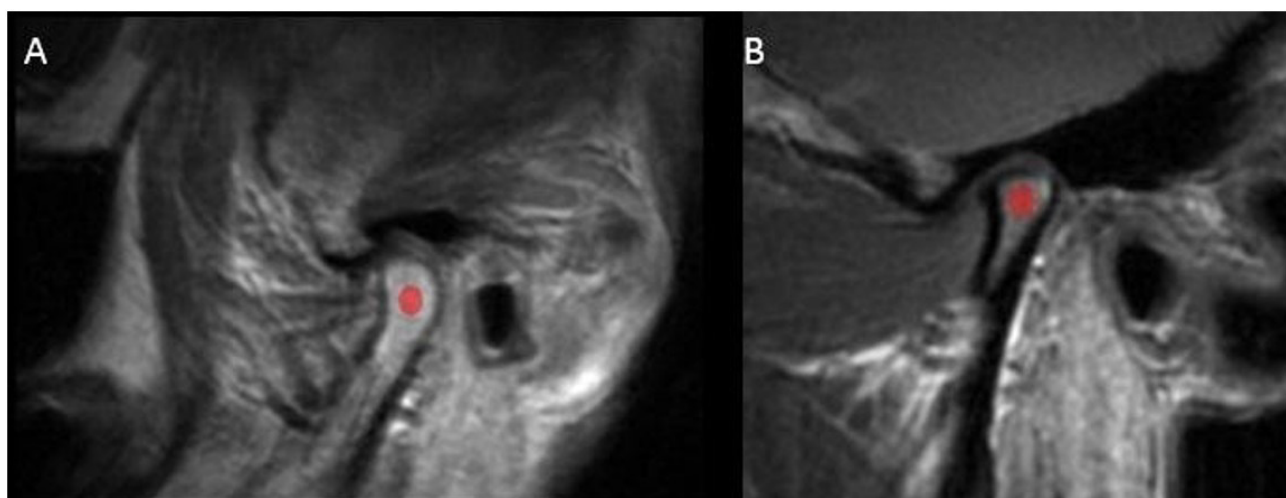


Figure 2 - Regions of interest established in the lateral pterygoid muscle in T2-weighted (A) and PD-weighted (B) magnetic resonance imaging reconstructions. Source: Prepared by the authors.

Table I - Sample Distribution in T2-weighted images

Weighted in T2	C (n)	TMD (n)
Lateral Pterygoid Muscle	20	20
Condylar Medullary Bone	20	20

Legend: C = control; TMD = temporomandibular disorder; n = sample size.
Source: Prepared by the authors.

Table II - Sample Distribution in Proton Density (PD)-weighted images

Weighted in PD	C (n)	TMD (n)
Lateral Pterygoid Muscle	20	20
Condylar Medullary Bone	20	20

Legend: C = control; TMD = temporomandibular disorder; n = sample size.
Source: Prepared by the authors.

The TA results were quantified using the GLCM. This approach is one of the six existing TA methods in the literature and This

approach is one of the six existing TA methods in the literature and operates by tabulating the occurrences of different combinations of pixel intensity values (gray levels) in an image [27]. The statistical parameters obtained from each GLCM are presented in Table III and illustrated in Figures 3 and 4.

Statistical analysis

The Mann-Whitney test was employed to compare the value of each texture parameter between the studied groups. Evaluations were conducted for intergroup comparisons. All *p*-values were adjusted using the Benjamin-Hochberg false discovery rate (FDR) procedure to correct for multiple tests [32,33]. The statistical significance level was set at a *p*-value < 0.05.

Table III - Description of the texture analysis parameters calculated through gray-level co-occurrence matrix method

Parameter	Description
Contrast (CO)	Represents the amount of local variation in gray values
Inverse Difference Moment (IDM)	Homogeneity of the distribution of image gray values
Angular Second Moment (ASM)	Measure of image uniformity
Correlation (COR)	Measures the linear dependence of gray values between neighboring pixels
Sum of Squares (SS)	Measure of dispersion (relative to the mean) of the distribution of gray values
Entropy (E)	Measures the degree of disorder among the image pixels
Sum of Average (SA)	Mean of the distribution of the sum of gray values
Sum of Variance (SV)	Dispersion around the mean of the distribution of the sum of gray values
Sum of Entropy (SE)	Measures the disorganization of the distribution of the sum of gray values
Difference of Variance (DV)	Measures the dispersion of the distribution of the difference of gray values
Difference of Entropy (DE)	Measures the irregularities associated with variations in the image gray values distribution

Source: Prepared by the authors.

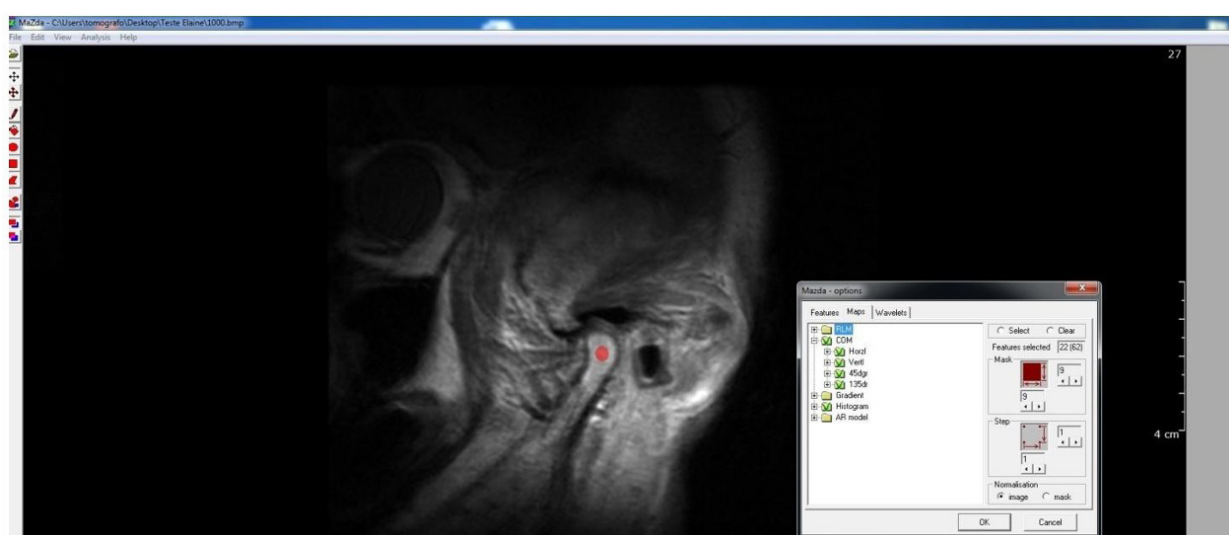


Figure 3 - Mazda software displaying: Selection of the parameters for the gray-level co-occurrence matrix (GLCM) method. Source: Prepared by the authors.

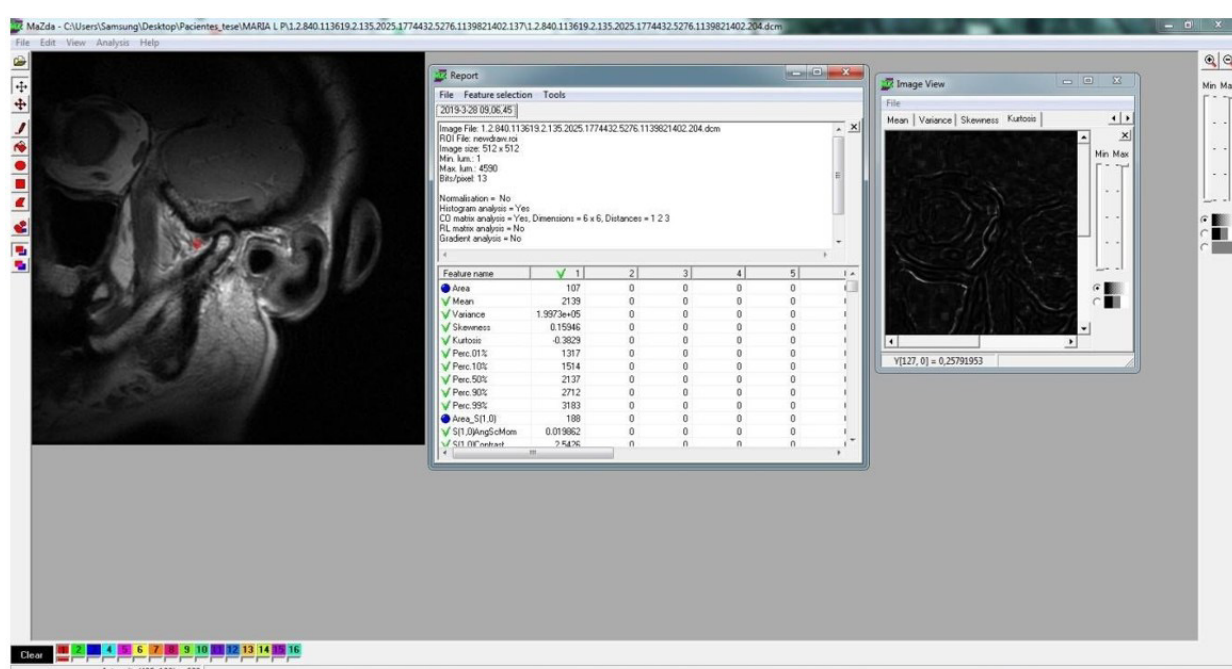


Figure 4 - Mazda software displaying: Outcomes of applying the gray-level co-occurrence matrix method. Source: Developed by the authors.

RESULTS

As shown in Table IV, a statistically significant difference was observed between the control and TMD groups concerning the inverse difference moment (IDM) parameter, as seen in T2-weighted images of the LPM region ($p < 0.05$). The IDM, serving as an indicator, reflects the homogeneity of the gray values distribution within the image.

Tables V, VI and VII present a summary of the intergroup analysis for the ROIs of the LPM and condylar medullary bone, respectively. No statistically significant difference was observed for the eleven parameters analyzed between the control and TMD groups in the T2-weighted images ($p > 0.05$).

As observed in Table VI, a statistically significant difference was noted between the

studied groups regarding the correlation (COR) parameter, an indicator of non-homogeneity in the distribution of gray values, particularly in the condylar medullary bone region in PD-weighted images. It is important to emphasize that no statistically significant differences were observed for the other parameters in the condylar medullary bone and LPM ROIs in PD-weighted images.

DISCUSSION

Several previous studies have employed the TA technique to characterize lesions in various regions of the body and to distinguish them from normal tissues [19].

McLaren et al. [18] employed TA in MRI scans, through GLCM, to detect and diagnose breast tumors. In a study focusing on brain

Table IV - Comparison between control (C) and temporomandibular disorder (TMD) groups for texture analysis parameters conducted in the region of interest (ROI) of the lateral pterygoid muscle (LPM) in proton density-weighted (PD) images

Parameter	LPM in DP	n	Mean	p-value
ASM	C	20	23.00	0.176
	TMD	20	18.00	
CO	C	20	17.85	0.152
	TMD	20	23.15	
COR	C	20	21.75	0.499
	TMD	20	19.25	
SS	C	20	19.65	0.646
	TMD	20	0.00	
IDM	C	20	24.35	0.037
	TMD	20	16.65	
SA	C	20	22.70	0.234
	TMD	20	18.30	
SV	C	20	19.85	0.725
	TMD	20	21.15	
SE	C	20	19.03	0.425
	TMD	20	0.00	
E	C	20	18.30	0.234
	TMD	20	22.70	
DV	C	20	18.25	0.224
	TMD	20	22.75	
DE	C	20	17.73	0.133
	TMD	20	23.28	

ASM = Angular Second Moment; CO = Contrast; COR = Correlation; SS = Sum of Squares; IDM = Inverse Difference Moment; SA = Sum of Average; SV = Sum of Variance; SE = Sum of Entropy; E = Entropy; DV = Difference of Variance; DE = Difference of Entropy; n = sample number; Mean = mean of the obtained values. Statistical significant p-value highlighted in bold ($p < 0.05$).

Source: Developed by the authors.

Table V - Comparison between control (C) and temporomandibular disorder (TMD) groups for texture analysis parameters conducted in the region of interest (ROI) of the lateral pterygoid muscle (LPM) in T2-weighted images

Parameter	LPM in T2	n	Mean	p-value
ASM	C	20	19.61	0.953
	TMD	20	19.39	
CO	C	20	19.68	0.919
	TMD	20	19.32	
COR	C	20	22.53	0.093
	TMD	20	16.47	
SS	C	20	20.42	0.609
	TMD	20	18.58	
IDM	C	20	19.47	0.988
	TMD	20	19.53	
SA	C	20	19.16	0.849
	TMD	20	19.84	
SV	C	20	20.79	0.474
	TMD	20	18.21	
SE	C	20	20.05	0.759
	TMD	20	18.95	
E	C	20	19.42	0.965
	TMD	20	19.58	
DV	C	20	20.11	0.737
	TMD	20	18.89	
DE	C	20	19.47	0.988
	TMD	20	19.53	

ASM = Angular Second Moment; CO = Contrast; COR = Correlation; SS = Sum of Squares; IDM = Inverse Difference Moment; SA = Sum of Average; SV = Sum of Variance; SE = Sum of Entropy; E = Entropy; DV = Difference of Variance; DE = Difference of Entropy; n = sample number; Mean = mean of the obtained values. Statistical significance level set at $p < 0.05$.

Source: Developed by the authors.

Table VI - Comparison between control (C) and temporomandibular disorder (TMD) groups for texture analysis parameters conducted in the region of interest (ROI) of the condylar medullary bone (CMB) in proton density-weighted (PD) images

Parameter	CMB in PD	n	Mean	p-value
ASM	C	20	19.88	0.735
	TMD	20	21.13	
CO	C	20	23.55	0.099
	TMD	20	17.45	
COR	C	20	16.40	0.027
	TMD	20	24.60	
SS	C	20	21.80	0.482
	TMD	20	0.00	
IDM	C	20	19.58	0.617
	TMD	20	21.43	
SA	C	20	22.20	0.358
	TMD	20	18.80	
SV	C	20	20.55	0.978
	TMD	20	20.45	
SE	C	20	21.05	0.766
	TMD	20	19.95	
E	C	20	21.65	0.534
	TMD	20	0.00	
DV	C	20	24.05	0.055
	TMD	20	16.95	
DE	C	20	23.50	0.105
	TMD	20	17.50	

ASM = Angular Second Moment; CO = Contrast; COR = Correlation; SS = Sum of Squares; IDM = Inverse Difference Moment; SA = Sum of Average; SV = Sum of Variance; SE = Sum of Entropy; E = Entropy; DV = Difference of Variance; DE = Difference of Entropy; n = sample number; Mean = mean of the obtained values. Statistical significant p-value highlighted in bold ($p < 0.05$).

Source: Developed by the authors.

tumors, Ditmer et al. [34] demonstrated the TA technique's ability to differentiate tissues by highlighting characteristics among lesions within the same tumor, including the quantification of intensity variations or surface patterns. In an investigation on the condylar cortex of the TMJ in Articular Osteoarthritis, Bianchi et al. [35], utilized bone imaging biomarkers, including GLCM, and observed the technique's effectiveness in detecting condylar bone degeneration. Additionally, Gonçalves et al. [13] explored changes in bone patterns related to periodontal disease using the TA technique with GLCM method in Cone Beam Computed Tomography images. The study's findings indicated the feasibility of distinguishing the affected area by comparing it to the normal pattern.

The TA method based on GLCM methodology employs texture parameters to highlight

Table VII - Comparison between control (C) and temporomandibular disorder (TMD) groups for texture analysis parameters conducted in the region of interest (ROI) of the condylar medullary bone (CMB) in T2-weighted images

Parameter	CMB in T2	n	Mean	p-value
ASM	C	20	17.92	0.381
	TMD	20	21.08	
CO	C	20	17.89	0.373
	TMD	20	21.11	
COR	C	20	22.55	0.090
	TMD	20	0.00	
SS	C	20	20.79	0.474
	TMD	20	18.21	
IDM	C	20	20.18	0.704
	TMD	20	18.82	
SA	C	20	19.89	0.827
	TMD	20	19.11	
SV	C	20	21.16	0.358
	TMD	20	17.84	
SE	C	20	20.08	0.748
	TMD	20	0.00	
E	C	20	19.74	0.895
	TMD	20	19.26	
DV	C	20	17.74	0.328
	TMD	20	21.26	
DE	C	20	18.05	0.422
	TMD	20	20.95	

ASM = Angular Second Moment; CO = Contrast; COR = Correlation; SS = Sum of Squares; IDM = Inverse Difference Moment; SA = Sum of Average; SV = Sum of Variance; SE = Sum of Entropy; E = Entropy; DV = Difference of Variance; DE = Difference of Entropy; n = sample number; Mean = mean of the obtained values. Statistical significance level set at $p < 0.05$.

Source: Developed by the authors.

disruptions in the homogeneity and uniformity of lesioned tissues in comparison to normal ones [14,23,34]. These parameters are effective for characterizing the gray-level distributions of ROIs, which, in turn, rely on the physical properties of the tissues depicted in the image.

In the current study, T2-weighted images were investigated, which are recommended when emphasizing joint effusion and bone marrow edema. Additionally, PD-weighted image sequences were employed, offering good spatial resolution for lesions in the articular disc and serving as an excellent option for distinguishing lateral and medial disc displacements [36].

In the assessment of T2-weighted images between the studied groups in this investigation (i.e. control and TMD groups), no statistically significant differences were found in the analyzed

parameters within the GLCM for both the condylar medullary bone and LPM. Despite these observed results, establishing a threshold for texture parameters is challenging, given the varied parameters displaying a tendency for statistical differences. It is concluded that the evaluation of joint effusion and bone marrow edema was inconclusive in this case, even though they may be present. However, further research with an expanded sample size could provide a more comprehensive comparison of these findings.

In the current study, it was observed that TA through the GLCM exhibited a statistically significant difference in differentiation between the studied groups. This distinction was evident in PD-weighted images for both the condylar medullary bone and LPM regions. The COR parameter, which assesses the measure of linear dependence in gray value levels between neighboring pixels in an image, showed statistically significant differences for the condylar medullary bone. This outcome may be associated with degenerative changes and condylar necrosis, detectable in relation to the physiology of the lesion in this region. In images with a certain local ordering of grayscale levels, the value of the COR parameter is high [37]. Therefore, the null hypothesis is rejected.

Additionally, the IDM parameter revealed a statistically significant difference in PD-weighted MRI images for the LPM region. This parameter measures the homogeneity of the gray values distribution in the image, which may be related to the presence of changes in this region, such as muscular fibrosis, serving as an image biomarker for assessing LPM in patients with TMD.

The results reported by Liu et al. [23], who employed TA to evaluate the LPM in patients with TMD using MRI scans, indicated a statistically significant difference in the contrast parameter. This parameter quantifies the local variation in gray values within an image. Consequently, the study concluded that this parameter can be regarded as an image biomarker for assessing the LPM in patients with TMD.

To the best of our knowledge, studies with objectives similar to those of the current investigation were not found. Nevertheless, Fardim et al. [24] explored goals somewhat akin to those proposed in our study. In their investigation involving patients with migraines, it was observed a potential influence of the migraine

on the behavior of TMJ disc displacements. High contrast values, low entropy values, and their correlation may correspond to displacements and a propensity for non-reduction of the disc in these individuals. Also, Muraoka et al. [38] sought to investigate the feasibility of TA using MRI images of the LPM in patients with rheumatoid arthritis affecting the TMJ. The seven analyzed parameters of the investigated region showed significant differences between the groups without and those with rheumatoid arthritis.

The small sample size is a relevant limitation of our study. Further studies using TA technique through MRI images for this purpose could be recommended, suggesting caution when analyzing the results. Therefore, this study holds significant clinical relevance by contributing to the evaluation of the condylar medullary bone and the LPM in patients with TMD through the application of TA on MRI images.

CONCLUSION

The characteristics of the TA technique applied to the condylar medullary bone and LPM regions, extracted through the GLCM in MRI images, can reveal and quantify whether these regions are altered when compared to normal conditions, as observed in PD-weighted images. Positive results obtained signify the potential of this tool as a more objective diagnostic aid for regions that share similarities in imaging appearance. However, further studies are needed in the future to assess the feasibility and solidify the importance of this tool in dentistry.

Author's Contributions

VGBO: Conceptualization; Writing – Original Draft Preparation, Data Curation. ECCBCA: Conceptualization; Data Curation; Investigation; Methodology; Resources; ALFC: Software; Writing – Review & Editing; Formal Analysis; MBM: Validation; Writing – Review & Editing. SLPCL: Conceptualization; Supervision; Validation; Visualization; Funding Acquisition; Formal Analysis; Writing – Review & Editing.

Conflict of Interest

The authors of the manuscript declare that there are no conflicts of interest.

Funding

This study was financed by the Coordenação de Aperfeiçoamento de Pessoal de Nível Superior - Brasil (CAPES) - Finance Code 001.

Regulatory Statement

This study was submitted and approved by the Research Ethics Committee (CEP)/Plataforma Brasil has approved this study under number: 4.151.640 / CAAE: 32339720.8.0000.0077.

REFERENCES

1. Oliveira SLS, Carvalho DS. Cefaléia e articulação temporomandibular. *Neurociencias*. 2002;10(3):141-52. <http://doi.org/10.34024/rnc.2002.v10.10307>.
2. Carrara SV, Conti PCR, Barbosa JS. Termo do 1º Consenso em Disfunção Temporomandibular e Dor Orofacial. *Dental Press J Orthod*. 2010;15(3):114-20. <http://doi.org/10.1590/S2176-94512010000300014>.
3. Contreras EFR, Fernandes G, Ongaro PCJ, Campi LB, Gonçalves DAG. Systemic diseases and other painful conditions in patients with temporomandibular disorders and migraine. *Braz Oral Res*. 2018;32(0):e77. <http://doi.org/10.1590/1807-3107bor-2018.vol32.0077>. PMid:30043839.
4. Gauer RL, Semidey MJ. Diagnosis and treatment of temporomandibular disorders. *Am Fam Physician*. 2015;91(6):378-86. PMid:25822556.
5. Santos PPA, Santos PRA, Souza LB. Características gerais da disfunção temporomandibular: conceitos atuais. *Rev Nav Odontol On Line*. 2009;3(1):10-3.
6. Calderon PS, Reis KR, Araújo CRP, Rubo JH, Conti PCR. Ressonância magnética nos desarranjos internos da ATM: sensibilidade e especificidade. *Rev Dent Press Ortodon Ortop Facial*. 2008;13(2):34-9. <http://doi.org/10.1590/S1415-54192008000200005>.
7. Montesinos GA, de Castro Lopes SLP, Trivino T, Sánchez JA, Maeda FA, de Freitas CF, et al. Subjective analysis of the application of enhancement filters on magnetic resonance imaging of the temporomandibular joint. *Oral Surg Oral Med Oral Pathol Oral Radiol*. 2019;127(6):552-9. <http://doi.org/10.1016/j.oooo.2018.11.015>. PMid:30587453.
8. Aiken A, Bouloux G, Hudgins P. MR imaging of the temporomandibular joint. *Magn Reson Imaging Clin N Am*. 2012;20(3):397-412. <http://doi.org/10.1016/j.mric.2012.05.002>. PMid:22877948.
9. Talmaceanu D, Lenghel LM, Bolog N, Hedesiu M, Buduru S, Rotar H, et al. Imaging modalities for temporomandibular joint disorders: an update. *Clujul Med*. 2018;91(3):280-7. <http://doi.org/10.15386/cjmed-970>. PMid:30093805.
10. Lopes SLPL. Outros métodos de exames por imagem. In: Campos FSF, Haite F No, editores. *Diagnóstico por Imagem em Odontologia*. Nova Odessa: Napoleão; 2018.
11. Bonilha L, Kobayashi E, Castellano G, Coelho G, Tinois E, Cendes F, et al. Texture analysis of hippocampal sclerosis. *Epilepsia*. 2003;44(12):1546-50. <http://doi.org/10.1111/j.0013-9580.2003.27103.x>. PMid:14636326.
12. Lubner MG, Smith AD, Sandrasegaran K, Sahani DV, Pickhardt PJ. CT texture analysis: definitions, applications, biologic correlates, and challenges. *Radiographics*. 2017;37(5):1483-503. <http://doi.org/10.1148/rg.2017170056>. PMid:28898189.
13. Gonçalves BC, Araujo EC, Nussi AD, Bechara N, Sarmento D, Oliveira MS, et al. Texture analysis of cone-beam computed tomography images assists the detection of furcal lesion. *J Periodontol*. 2020;91(9):1159-66. <http://doi.org/10.1002/JPER.19-0477>. PMid:32003465.
14. Oliveira MS, Fernandes PT, Avelar WM, Santos SL, Castellano G, Li LM. Texture analysis of computed tomography images of acute ischemic stroke patients. *Braz J Med Biol Res*. 2009;42(11):1076-9. <http://doi.org/10.1590/S0100-879X2009005000034>. PMid:19820884.
15. Oliveira MS, Betting LE, Mory SB, Cendes F, Castellano G. Texture analysis of magnetic resonance images of patients with juvenile myoclonic epilepsy. *Epilepsy Behav*. 2013;27(1):22-8. <http://doi.org/10.1016/j.yebeh.2012.12.009>. PMid:23357730.
16. Kassner A, Thornhill RE. Texture analysis: a review of neurologic MR imaging applications. *AJR Am J Neuroradiol*. 2010;31(5):809-16. <http://doi.org/10.3174/ajnr.A2061>. PMid:20395383.
17. Simpson AL, Adams LB, Allen PJ, D'Angelica MI, DeMatteo RP, Fong Y, et al. Texture analysis of preoperative CT images for prediction of postoperative hepatic insufficiency: a preliminary study. *J Am Coll Surg*. 2015;220(3):339-46. <http://doi.org/10.1016/j.jamcollsurg.2014.11.027>. PMid:25537305.
18. McLaren CE, Chen WP, Nie K, Su MY. Prediction of malignant breast lesions from MRI features: a comparison of artificial neural network and logistic regression techniques. *Acad Radiol*. 2009;16(7):842-51. <http://doi.org/10.1016/j.acra.2009.01.029>. PMid:19409817.
19. Raja JV, Khan M, Ramachandra VK, Al-Kadi O. Texture analysis of CT images in the characterization of oral cancers involving buccal mucosa. *Dentomaxillofac Radiol*. 2012;41(6):475-80. <http://doi.org/10.1259/dmfr/83345935>. PMid:22241875.
20. Zhang H, Li W, Hu F, Sun Y, Hu T, Tong T. MR texture analysis: potential imaging biomarker for predicting the chemotherapeutic response of patients with colorectal liver metastases. *Abdom Radiol*. 2019;44(1):65-71. <http://doi.org/10.1007/s00261-018-1682-1>. PMid:29967982.
21. Chen Z, Chen X, Liu M, Liu S, Yu S, Ma L. Magnetic resonance image texture analysis of the periaqueductal gray matter in episodic migraine patients without T2-visible lesions. *Korean J Radiol*. 2018;19(1):85-92. <http://doi.org/10.3348/kjr.2018.19.1.85>. PMid:29354004.
22. Lian MJ, Huang CL. Texture feature extraction of gray-level co-occurrence matrix for metastatic cancer cells using scanned laser pico-projection images. *Lasers Med Sci*. 2019;34(7):1503-8. <http://doi.org/10.1007/s10103-018-2595-5>. PMid:30043142.
23. Liu MQ, Zhang XW, Fan WP, He SL, Wang YY, Chen ZY. Functional changes of the lateral pterygoid muscle in patients with temporomandibular disorders: a pilot magnetic resonance images texture study. *Chin Med J (Engl)*. 2020;133(5):530-6. <http://doi.org/10.1097/CM9.0000000000000658>. PMid:32049744.
24. Fardim KAC, Ribeiro TMAM, Araújo ECCBC, Ogawa CM, Costa ALF, Lopes SLPC. Magnetic resonance imaging texture analysis of the temporomandibular joint for changes in the articular disc in individuals with migraine headache. *Braz Dent Sci*. 2023;26(1):e3649. <http://doi.org/10.4322/bds.2023.e3649>.
25. Dworkin SF, Le Resche L. Research diagnostic criteria for temporomandibular disorders review, criteria, examinations and specifications, critique. *J Craniomandibular Disorders Orofac Pain*. 1992;6(4):301-55.
26. Strzelecki M, Szczypinski P, Materka A, Klepaczko A. MaZda - A software tool for automatic classification and segmentation of 2D/3D medical images. *Nucl Instrum Methods Phys Res A*. 2013;702:137-40. <http://doi.org/10.1016/j.nima.2012.09.006>.

27. Szczypinski PM, Strzelecki M, Materka A, Klepaczko A. A software package for image texture analysis. *Comput Methods Programs Biomed.* 2008;94(1):66-76. <http://doi.org/10.1016/j.cmpb.2008.08.005>.
28. Szczypinski PM, Strzelecki M, Materka A. **Mazda: a software for texture analysis.** In: *Proceedings of the International Symposium on Information Technology Convergence (ISITC); 2007; Jeonju, Korea (South)*. New York: IEEE; 2007. p. 245-9. <http://doi.org/10.1109/ISITC.2007.15>.
29. Obuchowicz R, Nurzynska K, Obuchowicz B, Urbanik A, Piorkowski A. Caries detection enhancement using texture feature maps of intraoral radiographs. *Oral Radiol.* 2020;36(3):275-87. <http://doi.org/10.1007/s11282-018-0354-8>. PMid:30484214.
30. Rosa CS, Bergamini ML, Palmieri M, Sarmento DJS, de Carvalho MO, Ricardo ALF, et al. Differentiation of periapical granuloma from radicular cyst using cone beam computed tomography images texture analysis. *Helijon.* 2020;6(10):e05194. <http://doi.org/10.1016/j.heliyon.2020.e05194>. PMid:33088959.
31. Nussi A, Castro Lopes S, Rosa C, Gomes JPP, Ogawa CM, Braz-Silva PH, et al. In vivo study of cone beam computed tomography texture analysis of mandibular condyle and its correlation with gender and age. *Oral Radiol.* 2023;39(1):191-7. <http://doi.org/10.1007/s11282-022-00620-3>. PMid:35585223.
32. Benjamini Y, Hochberg Y. Controlling the false discovery rate: a practical and powerful approach to multiple testing. *J R Stat Soc Series B Stat Methodol.* 1995;57(1):289-300. <http://doi.org/10.1111/j.2517-6161.1995.tb02031.x>.
33. Mungai F, Verrone GB, Pietragalla M, Berti V, Addeo G, Desideri I, et al. CT assessment of tumor heterogeneity and the potential for the prediction of human papillomavirus status in oropharyngeal squamous cell carcinoma. *Radiol Med.* 2019;124(9):804-11. <http://doi.org/10.1007/s11547-019-01028-6>. PMid:30911988.
34. Ditmer A, Zhang B, Shuaat T, Pavlina A, Luibrand N, Gaskill-Shipley M, et al. Diagnostic accuracy of MRI texture analysis for grading gliomas. *J Neurooncol.* 2018;140(3):583-9. <http://doi.org/10.1007/s11060-018-2984-4>. PMid:30145731.
35. Bianchi J, Goncalves JR, Ruellas ACO, Vimort J-B, Yatabe M, Paniagua B, et al. Software comparison to analyze bone radiomics from high resolution CBCT scans of mandibular condyles. *Dentomaxillofac Radiol.* 2019;48(6):20190049. <http://doi.org/10.1259/dmfr.20190049>. PMid:31075043.
36. Ramos A, Sarmento V, Campos P, Gonzalez M. Articulação temporomandibular - aspectos normais e deslocamentos de disco: imagem por ressonância magnética. *Radiol Bras.* 2004;37(6):449-54. <http://doi.org/10.1590/S0100-39842004000600013>.
37. Haralick RM, Shanmugam K, Dinstein I. Textural features for image classification. *IEEE Trans Syst Man Cybern.* 1973;3(6):610-21. <http://doi.org/10.1109/TSMC.1973.4309314>.
38. Muraoka H, Kaneda T, Hirahara N, Ito K, Okada S, Kondo T. Magnetic resonance image texture analysis of the lateral pterygoid muscle in patients with rheumatoid arthritis: a preliminary report. *Oral Radiol.* 2023;39(2):242-7. <http://doi.org/10.1007/s11282-022-00625-y>. PMid:35701653.

Victoria Geisa Brito de Oliveira
(Corresponding address)

Universidade Estadual Paulista “Júlio de Mesquita Filho”, Instituto de Ciência e Tecnologia,
Departamento de Diagnóstico e Cirurgia, São José dos Campos, SP, Brazil.
Email: victoria.gb.oliveira@unesp.br

Date submitted: 2024 Mar 21
Accept submission: 2024 June 11